Noname manuscript No.
(will be inserted by the editor)

Unscented Kalman Filter Based Method for Spacecraft Navigation Using Resident Space Objects

Matthew Driedger · Michael Rososhansky · Philip Ferguson

Received: 28 June, 2019 / Accepted: date

Abstract The number of resident space objects (RSOs) in orbit has increased dramatically within the last ten years. While RSOs pose a serious challenge to our continued use of space, these objects also provide an opportunity to improve on-orbit state estimation. Spacecraft star trackers are commonly used to determine the orientation of its host spacecraft but these sensors are also capable of detecting RSOs. These detections contain orbital positional information that traditional star-images lack and could allow star trackers to provide both position and attitude state estimates.

In order for RSO-based optical navigation to be commercially viable, a reliable filter covariance estimate is required. This paper introduces an Unscented Kalman Filter (UKF) for estimating an observing spacecraft's position and attitude based on RSO observations. To ensure this filter is reliable, a technique for bounding the estimate error with the moving standard deviation of its error and the square root of its covariance is introduced. This method provides strong indicator for the reliability of an estimate.

In developing this work, several integrators were examined and an improvement was made for applying the Euler method to state estimation by adding the local truncation error (LTE) to the system's process noise. This addition provides a small but noticeable decrease in the number and magnitude of error spikes in the resulting state estimates and allows the method to perform better at larger time steps than the standard Euler method.

Keywords RSO based Optical Navigation · Unscented Kalman Filter · Optical Navigation · Spacecraft Navigation · Guidance, Navigation, and Control

Matthew Driedger
PhD Student
Department of Mechanical Engineering
University of Manitoba
E-mail: umdrie34@myumanitoba.ca

Michael Rososhansky
Senior Researcher in Estimation and Control
Department of Mechanical Engineering
University of Manitoba

Philip Ferguson
NSERC / Magellan Aerospace Industrial Research Chair in Satellite Engineering
Department of Mechanical Engineering
University of Manitoba

1 Introduction

Spacecraft navigation and controls engineers are accustomed to extracting data from multiple sources in an effort to accurately determine a spacecraft's attitude, attitude rates and orbital parameters [1]. Star trackers, gyros, accelerometers, sun sensors, earth horizon sensors, magnetometers and GPS receivers are all commonly used sensors used for spacecraft navigation and control.

The purpose of this research is to investigate new ways to obtain more performance out of less equipment, thereby reducing the overall cost and complexity of satellite missions. Specifically, by extracting more information from star trackers, satellite designers may be able to one day improve the navigational (both attitude and orbit) solution while simultaneously reducing the cadre of sensors required to complete a given mission.

Researchers such as Crassidis et al. [2] and Junkins et al. [3], have examined methods of optical spacecraft navigation, focusing on rendezvous and docking applications in which an observing spacecraft is less

than 100 meters from an observed-object. Hu et al. have explored the feasibility of using optical navigation at greater distances, examining how a satellite in low Earth orbit could use optical sightings of a reference satellite in geostationary Earth orbit to estimate the observer's state [4]. Previous research in optical navigation has relied on custom sensors such as VISNAV [3], but many satellites already include powerful optical navigation sensors in the form of star trackers.

Star trackers have had to become increasingly intelligent to reject "false" star images arising from glinting space objects in order to compensate for the increased density of resident space objects (RSOs). These algorithms attempt to identify non-star images and actively reject them prior to forwarding the starfield image to the guide star catalog correlator for identification [5]. Star trackers have become sophisticated enough that star trackers can be used as a tool for detecting and cataloging RSOs [6].

As space commerce continues to grow, so does the density of space assets in "popular" orbits (low earth orbit, polar orbits, sun synchronous orbits and geostationary orbits) [7]. These assets are largely comprised of spent rocket bodies and satellites (many have been inactive for years or decades). Similar to the meticulous measurements astronomers take to map the location of stars in the sky [8], space researchers and military organizations such as the United States Strategic Command measure and track orbital parameters of most RSOs larger than 5 cm in diameter [9], [10].

Using commercially available star trackers and reference objects from existing RSO databases, an observing satellite could use optical navigation techniques for orbit determination, similar the methods proposed by Hu [4]. On a small scale, the concept of using other space assets to assist in navigation is not new. Previous research has studied ways in which a fleet of cooperative spacecraft could decentralize their fleet state estimation (orbital determination) using GPS and local transmitters that measure the relative distance and velocity (using Doppler measurements) between pairs of spacecraft in the fleet [11], [12], [13].

Preliminary research has indicated that RSO-based optical navigation is possible, using a small number of reference objects in various orbits [14]. However, the non-linear and non-Gaussian nature of our measurement equation make using these measurements challenging. In our previous work, we used an Extended Kalman Filter (EKF) to estimate a simulated observer's state using a combination reference points modelling RSOs and stars. The Extended Kalman Filter is a popular method for estimating the state of non-linear dynamic systems and locally linearizes the system around its mean and covariance prior to predicting its state [15].

While our previous work was promising and the EKF converged onto a steady state, the estimator errors were not bounded by the convariance estimates. A major barrier to technology adoption and commercialization in the space industry is trust. Without a trustworthy metric (such as the estimated covariance), spacecraft designers are understandably cautious of new navigation schemes out of fear that the solution could unknowingly diverge, leading to catastrophic spacecraft failures. As a result, a better navigation solution than the EKF is required that provides a reliable covariance estimate. To this end, this paper examines the use of an Unscented Kalman Filter (UKF) for RSO-based optical navigation. Unlike the EKF, the UKF does not locally-linearize a system and so it is better suited to highly non-linear models [16], [17].

Reliability and predictability are key to the adoption of new technologies by the space industry [18]. To help gauge the reliability of our state estimates, we have calculated the moving standard deviations for all estimate errors. For a well-behaved filter, this 'true'standard deviation should be less than or equal to the standard deviation predicted by the filter (by the square root of the covariance).

In addition, we examine the effectiveness of several integrators, including an improvement for applying the Euler method to state estimation by adding the local truncation error (LTE) to the system's process noise as a means of capturing integration error as well as the typical unmodeled dynamics into the filter's process noise.

2 Problem Formulation

First, let us explore a simplified two-dimensional model of the relationship between an observer (the observing satellite attempting to use RSO and star measurements for navigation) and a detectable object (*e.g.*, an RSO or star).

Consider an observer moving in a circular path (or orbit) and a fixed object as shown in fig. 1. Our goal in this work is to estimate the position, attitude and rates of the observer using angular measurements between the observer and various objects.

The observer has a position of $r = [x, y]^T$ and an attitude angle of ϕ. The observer detects the relative angle θ between its local frame of reference and the fixed object. We assume that the observer has access to a database of objects and thus, we know the position of the object. Let the global position of the object be

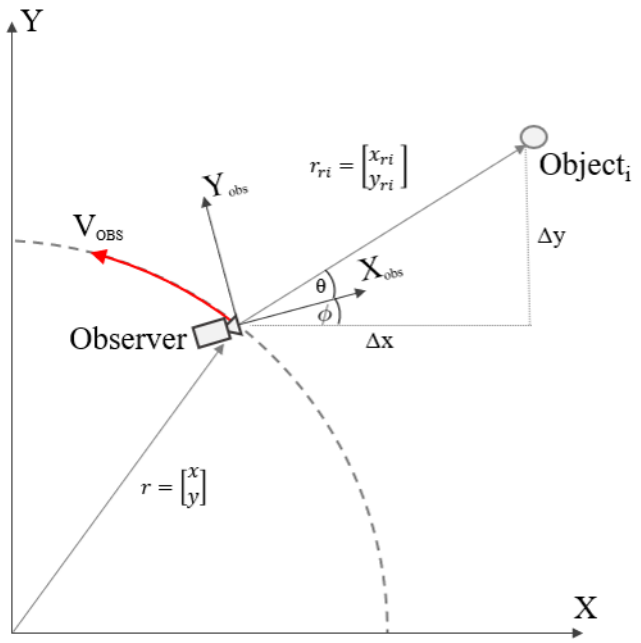

Fig. 1 An observer in a circular orbit detecting the angle between its internal reference frame and an external object i.

$r_{ri} = [x_{ri}, y_{ri}]^T$ and let $(\Delta x, \Delta y)$ denote the relative position of the object with respect to the observer. From fig. 1 we note that:

$$\tan(\theta + \phi) = \frac{\Delta y}{\Delta x} = \frac{y_{ri} - y}{x_{ri} - x} \tag{1}$$

Assuming that the position of the observed object is known, we can express the observed angle measurement θ as a function of the observed object's position and the observer's position:

$$\theta = \tan^{-1}\left[\frac{y_{ri} - y}{x_{ri} - x}\right] - \phi \tag{2}$$

The measurement θ mimics the measurement we would obtain from a star tracker. In reality, a star tracker would return the position of a centroided image on an imaging plane. However, for simplicity, we have assumed that this transformation between the imaging plane and the angle has already happened. It should be noted that this model also assumes that the observed objects are fixed and continually observable. Owing to the highly nonlinear natures of Equation 2, the resulting measurements from this model have a non-Gaussian distribution.

Note that the authors purposefully chose to develop this filter using two translational dimensions and one rotational dimension to keep the filters and underlying model simple and understandable. We believe that adding additional degrees of freedom will not have a significant effect the feasibility of this navigational method, nor would they change the covariance analysis that this paper presents.

3 Navigation Filter Design

The authors developed a series of filters based on the previously-described geometry of fig. 1 to determine a) if an observer's state can be estimated using the measurement equation (equation 2) and b) if the resulting filter covariance bounds the actual estimator error, as a means of providing confidence in the method. Continuing on previous work [14], an Unscented Kalman Filter (UKF) was used to estimate our observing satellite's state using Euler and 4^{th} order Runge-Kutta integration methods. We chose to use a UKF, per the methods of [20], as we believed that a UKF could accommodate our non-linear measurement estimate better than the previous EKF [19], leading to a more truthful covariance estimate. Additionally, we chose to examine the effects of Euler and 4^{th} order Runge-Kutta integration methods on the accuracy and trustworthiness of the filter.

The observer's state matrix X was defined, as seen in equation 3, including the observer's position and velocity in x and y as well as the observers attitude ϕ and rotational velocity $\dot{\phi}$.

$$X = \left[x \; y \; \dot{x} \; \dot{y} \; \phi \; \dot{\phi}\right]^T \tag{3}$$

As we have chosen to use Cartesian coordinates to describe the observer's dynamics in a circular orbit, the control force exerted on the observer in x and y is a function of its previous position:

$$F_x(t) = -\frac{4\pi^2 x^2}{mT^2|r|} \tag{4}$$

$$F_y(t) = -\frac{4\pi^2 y^2}{mT^2|r|} \tag{5}$$

Where F_x and F_y are the observer's accelerations in x and y respectively, x and y are the observer's position in an Earth-centric Cartesian coordinate system, T is the observer's orbital period, m is the observer's mass, and $|r|$ is the magnitude of the observer's position. Similarly, the torque applied to the observer was defined as shown in

$$\tau(t) = A\cos\left(\frac{2tn\pi}{T}\right) \tag{6}$$

Where A is the magnitude of the torque, n is the frequency, and T is the orbital period.

Neglecting process noise w, this results in the linear system of equations seen below:

$$X_t = \begin{bmatrix} x_0 + \frac{|v|xt}{|r|} + \frac{F_x t^2}{2m} \\ y_0 + \frac{|v|yt}{|r|} + \frac{F_y t^2}{2m} \\ \dot{x}_0 + \frac{F_x t}{m} \\ \dot{y}_0 + \frac{F_y t}{m} \\ \phi_0 + \dot{\phi} t + \frac{\tau t^2}{2J} \\ \dot{\phi}_0 + \frac{\tau t}{J} \end{bmatrix} \quad (7)$$

Where A is the magnitude of the torque, n is the frequency, and T is the orbital period, m is the observer's mass, $|v|$ is the magnitude of the observer's orbital velocity, J is its inertia, τ is the torque imparted onto the observer, and t is the sample time. As simplifications, mass m and particle inertia J were assumed to be 84 kg and 2.8 kg·m^2 respectively. An arbitrary sinusoidal torque with a magnitude of 5 μN·m was applied to the observer and time steps of 0.05 s were used. Equation 7 was integrated using both Euler and 4^{th} order Runge-Kutta methods so that the accuracy and computation time of both methods could be compared.

After these observer dynamics were integrated, "true" measurements were taken for each observed object and time step, using the previously described measurement equation (Equation 2). Sample measurements were obtained by adding a random normal standard deviation of 5 arc-seconds to the true measurements, to mimic the boresight accuracy of a commercially available nanosatellite star tracker [21]. This measurement noise was used to calculate the measurement noise covariance matrix R, as follows:

$$R = I_{n\times n} v^2 \quad (8)$$

Where v is the measurement noise standard deviation and $I_{n\times n}$ is an identify matrix where n is the number of measurement sources.

Process noise was applied as a random normal distribution with means equal to 1% of the applied force (7.4 N) for position-dynamics and 1% of the applied torque (0.05 μN·m) for attitude-dynamics. Using the above mentioned process noise, the process noise covariance was calculated using the Q evaluation process as described by Brown and Hwang [22].

An important part of this research is to determine the extent to which the filter can compute the confidence of a given estimate, expressed through the filter's covariance. As such, we have been meticulous about ensuring that the filter accurately represents the same (appropriately discretized) measurement and process noise used to create the truth data. Of course, in a real filter implementation, while filter designers usually have good knowledge of the sensor noise, they do not know the actual process noise and must estimate it based on an evaluation of unmodeled dynamics. For the purposes of this research, we are exploring how accurately our UKF tracks the covariance of the estimate when given perfect filter process and measurement noise covariances (R and Q).

3.1 Euler Truncation Error Compensation

As the Euler method is a first-order method, the local truncation error (LTE) introduced with every time step can be significant. As demonstrated by Simon [23], Euler integration can have a percent error of 1.3% for a time step of 0.05 seconds, compared to 2.2×10^{-7}% for a 4^{th} order Runge-Kutta method with the same time step. Errors of this size can become a non-negligible source of process noise such as in our case where we have defined our process noises to be 1% of our control input.

The filter can compensate for this integration error by including the LTE into its process noise. Assuming that the ordinary differential equation y being integrated has a continuous second derivative and the initial time is zero, the maximum LTE introduced into the system at each time-step can be expressed by equation (9) [25].

$$LTE = y(\Delta t) - y_1 \approx \frac{\Delta t^2 y'' \xi}{2} \quad (9)$$

Where Δt is the time step used, y'' is the equation's second derivative, and ξ is a constant with an upper bound of Δt. Assuming that ξ is at this upper bound, the maximum LTE for each element of our state function can be expressed as:

$$LTE = \frac{\Delta t^3 X_t''}{2} = \frac{\Delta t^3}{2} \begin{bmatrix} \gamma|r| + |v|\Delta t\gamma + \gamma^2 \Delta t^2 |r| \\ \gamma|r| + |v|\Delta t\gamma + \gamma^2 \Delta t^2 |r| \\ \gamma^2|r| \\ \gamma^2|r| \\ \frac{A(T^2 - 2n^2\pi^2 t^2)}{JT^2} \\ \frac{-4\pi^2 n^2 A \Delta t}{T^2 J} \end{bmatrix} \tag{10}$$

Where X'' is the second derivative of the state matrix and γ is:

$$\gamma = \frac{4\pi^2}{T^2} \tag{11}$$

4 Simulation Results

To evaluate the performance of the UKF filter, we simulated an observing spacecraft in a 400 km circular orbit which observed a set of fixed beacons using the measurement equation (equation 2). Since our measurement equation was non-Gaussian, we set the UKF tuning parameters κ and β to 2 and 0 respectively, as recommended by Turner and Rasmussen [24]. α was set to 5×10^{-4}.

All tests were performed using time steps of 0.05 seconds, and the initial state estimates for each filter were set to zeros. Twelve measurement sources were used for each test: four fixed beacons at distances of 10^{12} meters from the centre of the observer's orbit to approximate stars, four beacons at distances of 8×10^6 meters, and four beacons at distances of 3×10^7 meters to approximate RSOs.

Figures 2, 3, and 4 show that the UKF filter was able to converge on very similar positional estimates with all three integration methods. The square roots of the covariances were found by taken the diagonal elements of the square root of the covariance matrix. I.E.:

$$\sigma = I_{m \times m} \sqrt{P} \tag{12}$$

Where σ is the predicted standard deviation, $I_{m \times m}$ is an identity matrix where m is the number of elements in the state matrix, and P is the state covariance.

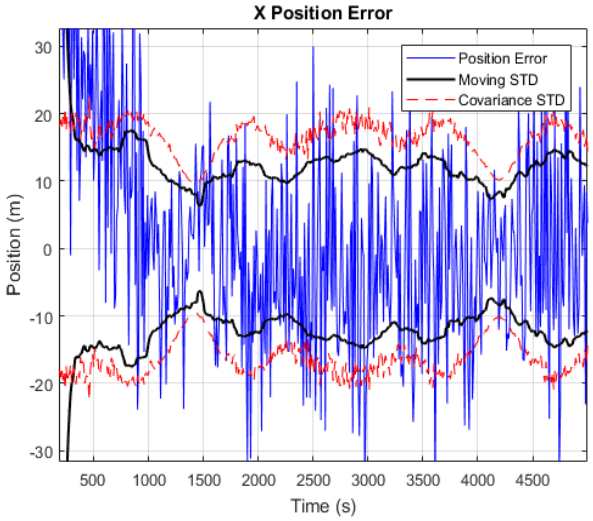

Fig. 2 X position error when using a UKF with an uncompensated Euler integration method.

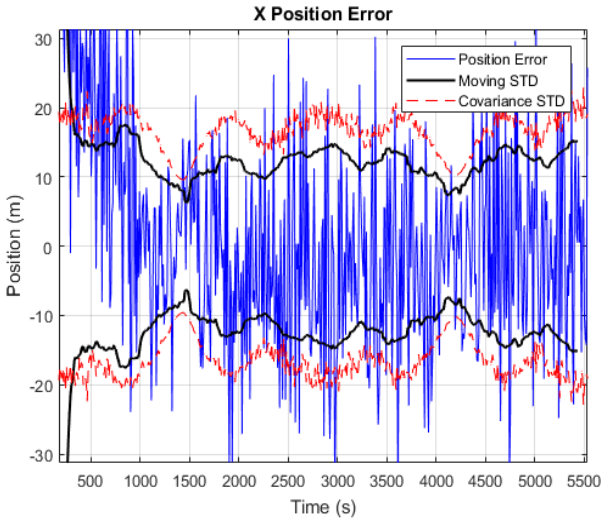

Fig. 3 X position error when using a UKF with an Euler integration method with local truncation error compensation.

While the results from all three UKF variants converged similarily, the three velocity error plots, presented in figures 5, 6, and 7, show that adding LTE compensation reduced the magnitude of error spikes and resulted in a similar performance to the 4^{th} order Runge-Kutta method. As expected, the 4^{th} order Runge-Kutta method performed the best of the three integrators but it's performance was comparable to the less-computationally-expensive Euler method when LTE compensation was added. Note that in all cases, the moving error standard deviation was bounded by the covariance.

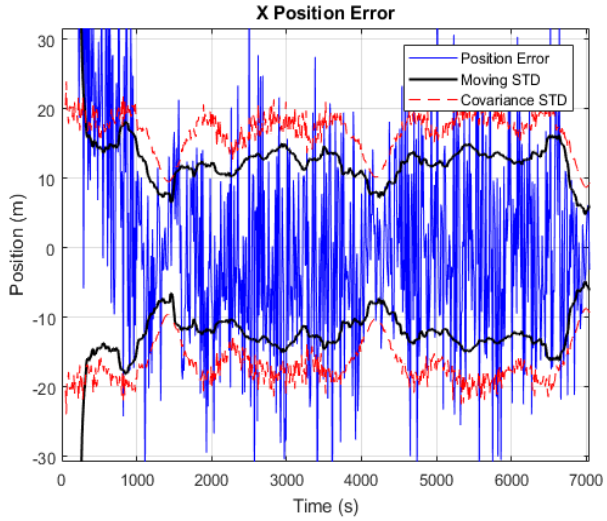

Fig. 4 X position error when using a UKF with a 4^{th} order Runge-Kutta integration method.

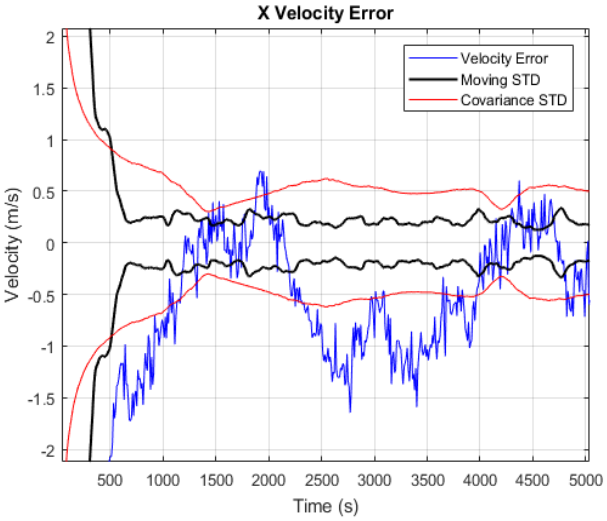

Fig. 5 X velocity error when using a UKF with an uncompensated Euler integration method.

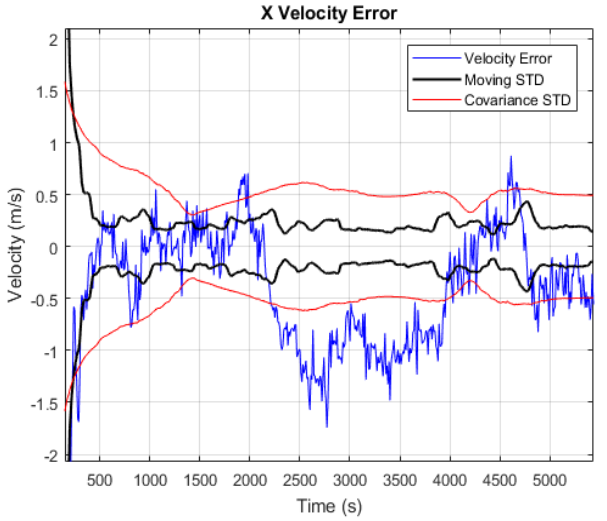

Fig. 6 X velocity error when using a UKF with an Euler integration method with local truncation error compensation.

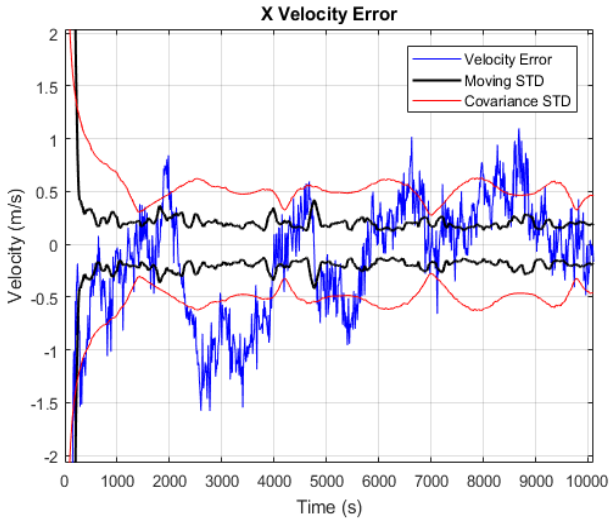

Fig. 7 X velocity error when using a UKF with a 4^{th} order Runge-Kutta integration method.

5 Discussion

As seen in the simulation results, all three versions of the UKF were capable of converging onto full state estimates within comparable time frames. After an initial settling period, all three methods reached steady-states in which their errors and the moving standard deviations of these errors were bounded by their covariance-based standard deviations. This is to be expected for a well-functioning filter, as the covariance-bounds form the filter's prediction of the estimate uncertainty while the moving standard deviation is the true uncertainty within the system. In contrast, the moving standard deviations were not bounded by the covariance for the Extended Kalman Filter used in our previous work, as seen in figure 14. This filter was unable to converge without artificially increasing the process noise covariance, as discussed in [14]. This suggests that standard deviation bounding may be a good metric to evaluate the reliability of a filter estimate.

A comparison of the Euler and Euler with LTE compensation integrators suggests that adding LTE compensation provides a small but noticeable decrease in the number and magnitude of error spikes. To explore this further, we re-ran both filters with a time step of 0.5 seconds. Figures 15 and 16 demonstrate that including truncation error compensation provides a more noticeable improvement on the filter's performance at larger time steps. However, this improved accuracy is still less

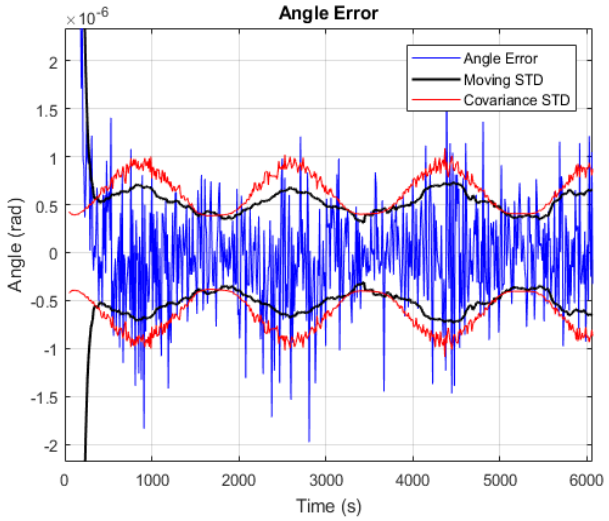

Fig. 8 Angle error when using a UKF with an uncompensated Euler integration method.

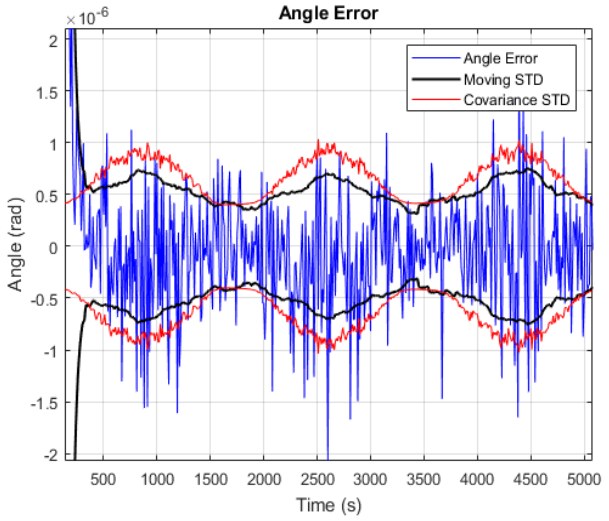

Fig. 9 Angle error when using a UKF with an Euler integration method with local truncation error compensation.

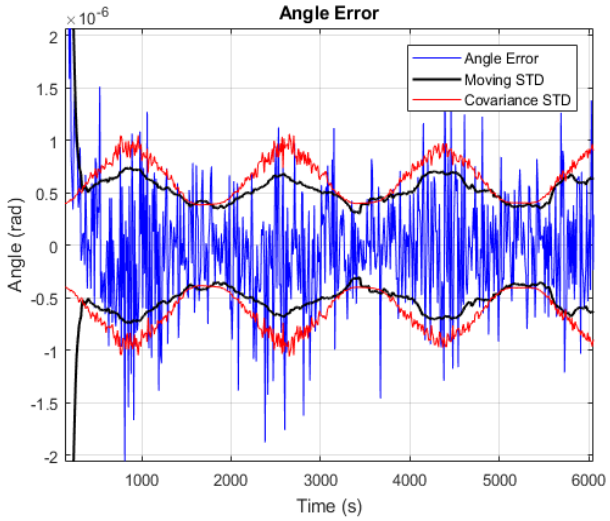

Fig. 10 Angle error when using a UKF with a 4^{th} order Runge-Kutta integration method.

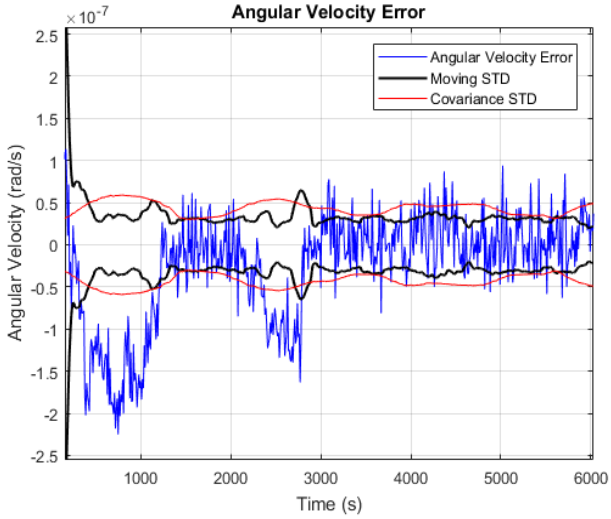

Fig. 11 Angular velocity error when using a UKF with an uncompensated Euler integration method.

than that of the 4^{th} order Runge-Kutta method and was insufficient to prevent the EKF from diverging.

6 Conclusion

This paper has presented improvements towards developing an RSO-based optical navigation technique for determining a satellite's position and attitude using RSO observations. The Unscented Kalman Filter developed here is an improvement on previous work for RSO-based optical navigation as the resulting state estimates remain bounded both by the moving standard deviation of its error and the square root of its covariance. The 'true'error standard deviation, calculated using the moving standard deviation, is less than the square root of the covariance for all cases and state elements and is a strong indicator that the resulting measurements can be reliably trusted.

In developing this work, several integrators were examined and an improvement was made for applying the Euler method to state estimation by adding the local truncation error (LTE) to the system's process noise. This addition provides a small but noticeable decrease in the number and magnitude of error spikes in the resulting state estimates and allows the method to perform better at larger time steps than the standard Euler method.

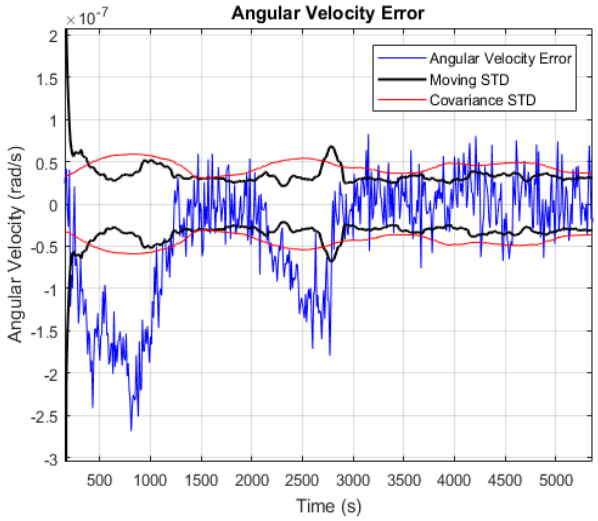

Fig. 12 Angular velocity error when using a UKF with an Euler integration method with local truncation error compensation.

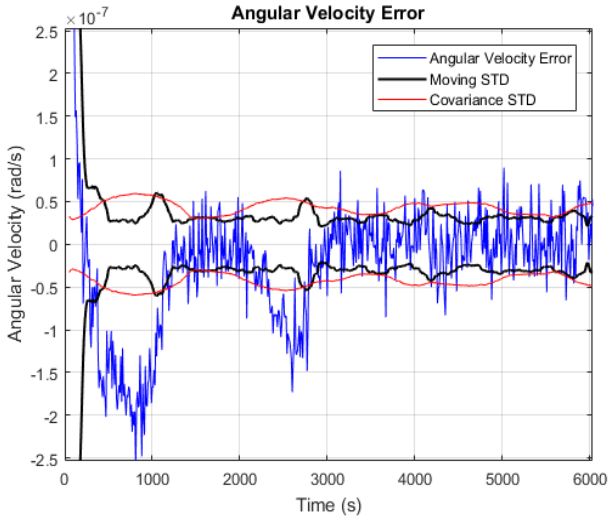

Fig. 13 Angular velocity error when using a UKF with a 4^{th} order Runge-Kutta integration method.

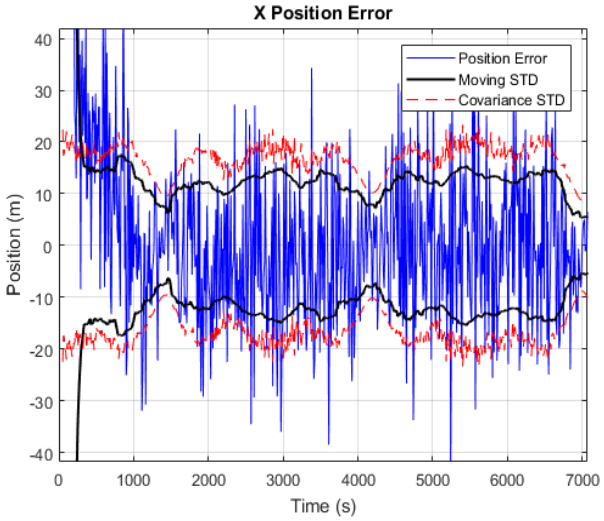

Fig. 14 Non-converging x position error when using an EKF with 4^{th} order Runge-Kutta integrator.

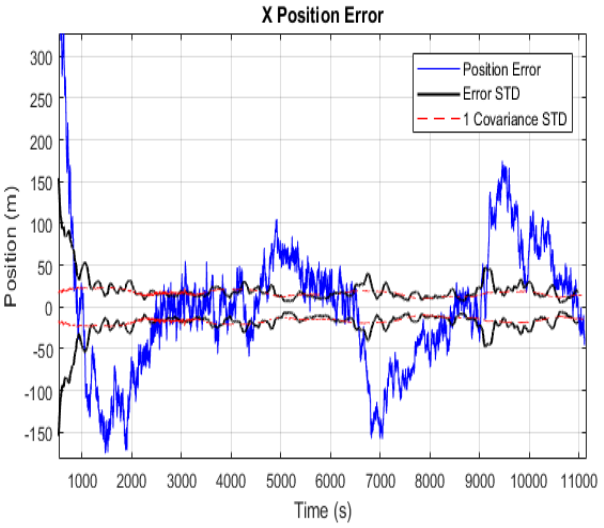

Fig. 15 X position error when using a UKF with an Euler integration method and a time step of 0.5 seconds.

7 Acknowledgments

The authors thank the Natural Sciences and Engineering Research Council (NSERC) of Canada, the Canadian Space Agency, and Magellan Aerospace for supporting this research.

References

1. E.J. Lefferts, F.L Markley, and M.D. Shuster, Kalman filtering for spacecraft attitude estimation, Journal of Guidance, Control, and Dynamics vol. 5 no. 5, pp. 417-429 (1982)
2. J. L. Crassidis, R. Alonso, J. L. Junkins, Optimal Attitude and Position Determination from Line-of-Sight Measurements, Journal of Astronautical Sciences, vol. 48 no. 2, pp. 391-408 (2000)
3. J. L. Junkins, D. C. Hughes, K. P. Wazni, V. Pariyapong, Vision Based Navigation for Rendezvous, Docking and Proximity Operations, 22nd Annual AAS Guidance and Control Conference, Breckenridge (1999)
4. Y. Hu, X. Bai, L. Chen, H. Yan, A new approach of orbit determination for LEO satellites based on optical tracking of GEO satellites, Aerospace Science and Technology, vol. 84 no. pp. 821-829 (2019)
5. J. Darling, N. Houtz, C. Frueh, and K. DeMars, Recursive Filtering of Star Tracker Data, AIAA/AAS Astrodynamics Specialist Conference, Long Beach, California (2016)
6. S. Clemens, R. Lee, P. Harrison, W. Soh, Feasibility of Using Commercial Star Trackers for On-Orbit Resident Space Object Detection, Advanced Maui Optical and Space Surveillance Technologies Conference (2018)
7. J.C. Liou et al., The new NASA orbital debris engineering model ORDEM2000, Space Debris, vol 473, (2001)

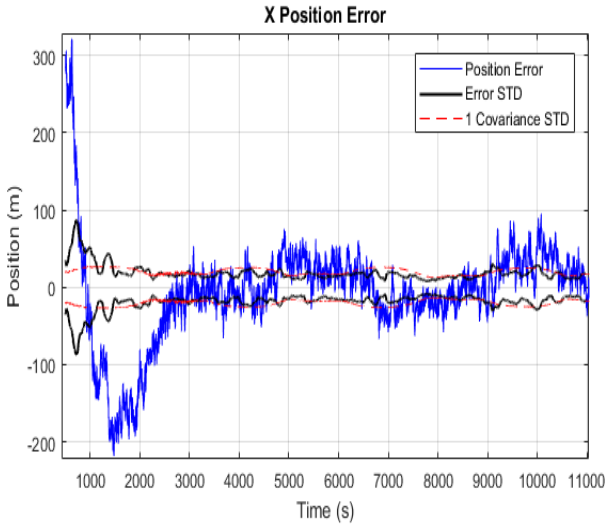

Fig. 16 X position error when using a UKF with an Euler integration method with local truncation error compensation and a time step of 0.5 seconds.

8. B.M. Lasker, et al., The second-generation guide star catalog: description and properties, The Astronomical Journal, vol. 136 no. 2, pp. 735 (2008)
9. P. Maskell and L. Oram, Sapphire: Canada's answer to space-based surveillance of orbital objects, Advanced Maui Optical and Space Surveillance Conference, (2008)
10. N.C. Anheier and C. Chen, A New Approach to Space Situational Awareness using Small Ground-Based Telescopes, No. PNNL- 23994, Pacific Northwest National Laboratory, Richland, WA (US), (2014)
11. C.W. Park, P. Ferguson, N. Pohlman, and J. P. How, Decentralized relative navigation for formation flying spacecraft using augmented CDGPS, In Proceedings of Institute of Navigation GPS Conference, Salt Lake City, UT (2001)
12. P. Ferguson and J. How, Decentralized estimation algorithms for formation flying spacecraft, In Proceedings of AIAA Guidance, Navigation and Control Conference (2003)
13. P. Ferguson, Distributed estimation and control technologies for formation flying spacecraft, PhD Thesis, Massachusetts Institute of Technology, Cambridge (2003)
14. M. Driedger and P. Ferguson, Orbital Navigation Using Resident Space Object Observations, Proceedings of the 2018 Small Satellite Conference, Logan Utah (2018)
15. G. Welch and G. Bishop, An introduction to the Kalman filter, Univ. North Carolina, Chapel Hill (2001)
16. S. J. Julier, J. K. Uhlmann, A new extension of the Kalman filter to nonlinear systems, In Proc. of AeroSense: The 11th Int. Symp. on Aerospace/Defence Sensing, Simulation and Controls (1997)
17. M. Rososhansky, Nonlinear Attitude And Formation Estimation Spacecraft And Multi-Agent Systems, PhD Thesis, Ryerson University, Toronto (2017)
18. P. Ferguson, Making Space for Everyone: a Research Program Aimed at Breaking Down Barriers to New Technology Adoption in Space, CASI ASTRO, Quebec City (2018)
19. E. A. Wan and R. van der Merwe, The Unscented Kalman Filter for Nonlinear Estimation, Proceedings of the IEEE 2000 Adaptive Systems for Signal Processing, Communications, and Control Symposium, Lake Louise (2000)
20. A. Gelb, Applied optimal estimation, MIT press (1974)
21. Second Generation Star Tracker (ST-16RT2), Sinclair Interplanetary (2017)
22. R. G. Brown and P. Y. C. Hwang, Introduction to Random Signals and Applied Kalman Filtering 3rd Ed., pp. 204, John Wiley & Sons, New York (1997)
23. D. Simon, Optimal State Estimation, pp. 33, John Wiley & Sons, New York (2006)
24. R. Turner and C. E. Rasmussen, Model Based Learning of Sigma Points in Unscented Kalman Filtering, 2010 IEEE International Workshop on Machine Learning for Signal Processing, Kittila (2010)
25. K. A. Atkinson, Kendall, An Introduction to Numerical Analysis (2nd ed.), pp. 342, John Wiley & Sons, New York (1989)